JOURNAL OF MAGNETIC RESONANCE 96, 215–221 (1992)

A 3D Triple-Resonance NMR Technique for Qualitative Measurement of Carbonyl–Hβ *J* Couplings in Isotopically Enriched Proteins

STEPHAN GRZESIEK,* MITSUHIKO IKURA, G. MARIUS CLORE, ANGELA M. GRONENBORN, AND AD BAX

Laboratory of Chemical Physics, National Institute of Diabetes and Digestive and Kidney Diseases, National Institutes of Health, Bethesda, Maryland 20892

Received August 27, 1991

It is well known that the magnitude of heteronuclear long-range couplings contains useful information regarding molecular conformation (*1*). For measurement of such couplings between protons and protonated heteronuclei, E.COSY-based techniques (*2*) in principle can yield quantitative results in isotopically enriched proteins (*3–6*). For measurement of *J* couplings to nonprotonated heteronuclei, deconvolution of the cross-peak shape in a ^{1}H-detected heteronuclear multiple-bond correlation (HMBC) spectrum (*7*) can be used (*8–10*), although for larger proteins the ^{1}H linewidth and extensive spectral overlap render this approach difficult, if not impossible.

Alternatively, qualitative information about the size of a long-range coupling can be obtained from the intensity of correlations in a 3D spectrum in which magnetization is transferred via the long-range coupling of interest. This has recently been demonstrated for couplings between ^{15}N and intraresidue Hβ protons (*11, 12*). Here we present an analogous experiment that uses magnetization transfer via the *J* coupling between the carbonyl (CO) and the Hβ protons. The resulting information about the CO–Hβ coupling, in combination with knowledge of the Hβ–^{15}N *J* coupling and qualitative (*13*) or quantitative (*2*) data on the Hα–Hβ couplings, allows unambiguous stereospecific assignment of the Hβ methylene protons and determines the rotomeric state of the Cα–Cβ bond (χ_1 angle).

The pulse sequence of our new experiment, which relies on magnetization transfer via the multiple-bond ^{1}H–^{13}CO *J* coupling, is sketched in Fig. 1. Because its main function is to correlate amide protons and ^{15}N nuclei to Hβ protons, using relay via the CO ^{13}C nucleus, we name the experiment HN(CO)HB. In this experiment, amide proton magnetization is transferred via its directly bonded ^{15}N nucleus to the adjacent carbonyl spin. A subsequent HMQC (*14–16*) segment correlates ^{13}CO with the Hβ protons and finally ^{13}CO magnetization is transferred back to the amide proton for detection. As recently shown for the triple-resonance HNCO experiment (*17, 18*), magnetization transfer from the amide proton to the carbonyl is quite efficient and uniform because this transfer takes place via large and well-resolved one-bond cou-

* On leave from F. Hoffmann–LaRoche Ltd., Basel, Switzerland.

0022-2364/92 $3.00

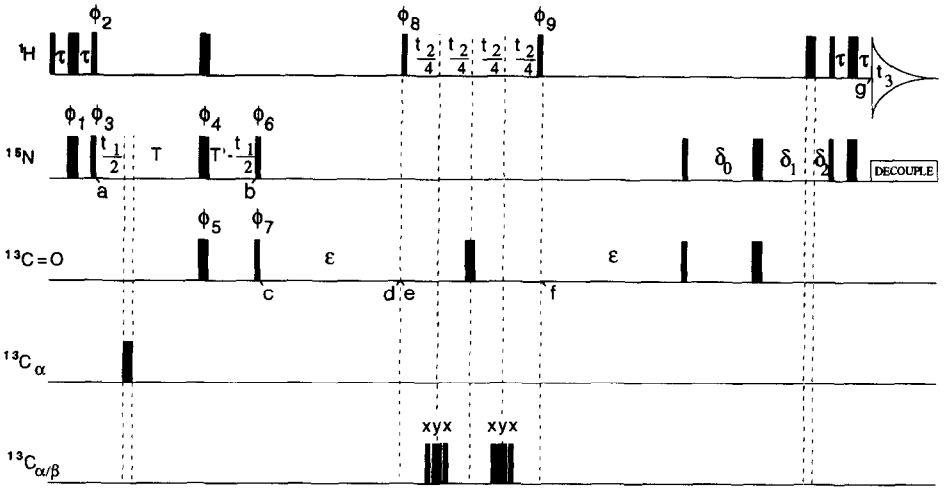

FIG. 1. Pulse scheme of the HN(CO)HB experiment. Narrow pulses correspond to a 90° flip angle and wide pulses correspond to 180°. Pulses for which the phase is not indicated are applied along the x axis. Phases and phase cycling of the other pulses are as follows: $\phi_1 = x, -x$; $\phi_2 = y, -y$; $\phi_3 = x$; $\phi_4 = 4(x), 4(y), 4(-x), 4(-y)$; $\phi_5 = 16(x), 16(-x)$; $\phi_6 = 8(x), 8(-x)$; $\phi_7 = x, x, -x, -x$; $\phi_8 = 16(x), 16(-x)$; $\phi_9 = 4(x), 8(-x), 4(x)$; Acq. $= 4(x, -x, -x, x), 4(-x, x, x, -x)$. Quadrature in the t_1 dimension is obtained by altering the phase ϕ_3 in a States–TPPI manner (*27*), and similarly, ϕ_8 is altered in a States–TPPI manner for quadrature detection in the t_2 dimension. Delay durations used are as follows: $\tau = 2.25$ ms; $T = 13.5$ ms; $T' = T + \tau_{180°}(C\alpha)$, where $\tau_{180°}(C\alpha)$ is the duration of the 180° $C\alpha$ pulse (162 μs); $\epsilon = 25$ ms; $\delta_0 = 10$ ms $+ \tau_{180°}(^1H)$, with $\tau_{180°}(^1H) = 21$ μs; $\delta_1 = 7.25$ ms; $\delta_2 = 2.75$ ms. $C\alpha$ pulses were applied at a frequency corresponding to 56 ppm; $C\alpha/\beta$ composite ($90°_x$ $180°_y$ $90°_x$) 180° pulses were applied at 44.5 ppm, with the RF power adjusted to give a 48.5 μs 90° pulse (yielding a null at the CO frequency for a ^{13}C spectrometer frequency of 151 MHz) and the carbonyl carrier was set at 177 ppm. The ^1H carrier is positioned on the H_2O resonance and H_2O presaturation is used.

plings. As will be discussed below, correlating the carbonyl with the Hβ resonances results in an approximate $(^3J_{CO-H\beta})^2$ dependence for the cross-peak intensity, thereby providing the information of interest.

First, we briefly outline the relevant magnetization-transfer steps, using the product-operator formalism to describe the spin system. For clarity, relaxation terms are not included and constant multiplicative factors are omitted. Only terms that result in observable magnetization during the detection period, t_3, are retained. The spin operators used are I for the amide proton, N for the amide ^{15}N, S for the carbonyl ^{13}C, and B for the Hβ proton. J_{XY} denotes the J coupling between spins X and Y, which is always a one-bond coupling except for J_{SB} and J_{Sk}, which denote a three-bond Hβ–CO J coupling and a multiple-bond J coupling between CO and a proton k, respectively. RF phases correspond to the first step of the phase cycle given in the legend to Fig. 1.

Longitudinal amide-proton magnetization (I_z), present at the start of the experiment, is transferred by means of an INEPT sequence into antiphase ^{15}N magnetization, yielding

$$\sigma_a = N_y I_z \cos(2\pi J_{NI}\tau). \qquad [1]$$

The following ^{15}N evolution period, t_1, is of the constant-time variety (*19–21*). Because the ^1H and ^{15}N 180° pulses are applied simultaneously during this "constant-time" interval ($T + T'$), the evolution due to J_{NH} coupling is not affected. Its total duration ($T + T'$) is chosen to be an odd multiple of $1/(2J_{NH})$ (27 ms in our experiment), such that the ^{15}N magnetization at the end of the t_1 evolution period (time b) is in phase with respect to spin I. The $180^\circ_{\phi 5}$ (CO) pulse is applied simultaneously with the $180^\circ_{\phi 4}$ (^{15}N) pulse to ensure that the ^{15}N magnetization becomes antiphase with respect to the carbonyl spin, S. The power and duration of the carbonyl 180° pulse are carefully adjusted in such a manner that the Cα resonances do not experience this pulse; i.e., for $t_1 = 0$, the ^{15}N spin remains in phase with respect to J-coupled Cα nuclei. A 180° Cα pulse applied during the constant-time evolution period ensures that the ^{15}N magnetization remains in phase with respect to Cα, independent of the t_1 value. At the end of the constant-time evolution period (time b) the relevant magnetization is described by

$$\sigma_b = N_y S_z \cos(2\pi J_{NI}\tau)\sin(2\pi J_{NS}T)\cos(\Omega_N t_1), \qquad [2]$$

where Ω_N denotes the ^{15}N angular offset frequency. Omitting the trigonometric terms, at time c one obtains

$$\sigma_c = N_z S_y. \qquad [3]$$

During the following intervals, between times c and d, the carbonyl magnetization remains in the transverse plane, but because of the 180° pulse applied at the middle of t_2, its chemical shift does not need to be taken into account. During the time ϵ, between time points c and d, S-spin magnetization becomes antiphase with respect to its long-range coupled protons. During the ϵ delay, the S-spin magnetization also dephases because of J coupling to the adjacent Cα and ^{15}N spins. However, the ^{13}CO dephasing caused by these interactions is also refocused at the end of the second ϵ interval and therefore may be ignored. Thus, at time d one obtains

$$\sigma_d = N_z S_x B_z \sin(\pi J_{SB}\epsilon) \prod_k \cos(\pi J_{Sk}\epsilon), \qquad [4]$$

which is converted into S–B multiple-quantum coherence by the subsequent ^1H $90^\circ_{\phi 8}$ pulse,

$$\sigma_e = N_z S_x B_y, \qquad [5]$$

where the trigonometric terms again have been omitted temporarily.

During both the first half and the second half of the t_2 evolution period, dephasing of the B_y term in expression [5] by coupling to its directly attached ^{13}C nucleus is prevented by the (composite) 180° pulses applied to the Cα and Cβ resonances. To avoid the necessity for large first-order phase corrections in the F_2 dimension of the spectrum, these pulses are applied only for durations of $t_2/2$ that are larger than the duration of the composite 180° Cα/β pulse (194 μs). The effect of S-spin resonance offset is removed by the 180° (CO) pulse applied at the midpoint of t_2. Note that one cannot use a single 180° Cα/β pulse to remove J coupling to proton B, because this would reintroduce the effect of the CO–Cα J coupling. At the end of the t_2 evolution

period the S–B multiple-quantum coherence is converted back into antiphase S-spin magnetization,

$$\sigma_f = N_z S_x B_z \cos(\Omega_B t_2), \quad [6]$$

where Ω_B denotes the angular offset frequency of proton B. The transfer of σ_f back into observable amide-proton magnetization follows the reverse pathway from that described above.

After the relevant trigonometric terms are reintroduced, the magnetization at the beginning of the detection period is described by

$$\sigma_g = I_x \cos^2(2\pi J_{NI}\tau)\sin(2\pi J_{NS}T)\cos(\Omega_N t_1)\cos(\Omega_B t_2) \times \sin[\pi(\delta + \delta_1 + \delta_2)J_{NS}]\sin^2(\pi J_{SB}\epsilon)\prod_k \cos^2(\pi J_{Sk}\epsilon). \quad [7]$$

^1H–^{15}N J couplings in proteins are all close to ~92 Hz and J_{NS} values are also quite uniform, varying from 13 to 16.5 Hz (*22*). Therefore, the sine and cosine terms containing J_{NS} and J_{NI} in expression [7] may be considered constants. To evaluate the attenuation caused by the $\cos^2(\pi J_{Sk}\epsilon)$ terms in Eq. [7], some knowledge of the magnitude of these couplings is required. Hansen *et al.* (*23*) report $^2J_{CO\text{–}H\alpha}$ couplings in the range of 4.2–7.1 Hz. Interresidue $^3J_{CO\text{–}H\alpha}$ couplings are usually smaller than 4 Hz, except for the rare case where the intervening N–Cα dihedral angle is close to +60° [corresponding to a trans orientation of CO(i) relative to Hα(i + 1)]. For the intraresidue $^3J_{CO\text{–}H\beta}$ coupling, Hansen *et al.* suggest a trans $^3J_{CO\text{–}H\beta}$ value of 11.9 Hz and a gauche value of 0.4 Hz. Bermel *et al.* (*8*) utilize less extreme values of 8.5 and 1.4 Hz, respectively. Considering that, to the best of our knowledge, no $^3J_{CO\text{–}H\beta}$ coupling larger than 8 Hz has ever been measured in a polypeptide, an upper limit of ~8 Hz for this coupling appears reasonable. Using an ϵ delay of 25 ms, passive couplings of 4 and 8 Hz cause an attenuation of 9 and 35% in cross-peak intensity, respectively. Hence, significant attenuation can be caused by these passive couplings. When the CO–Hβ connectivity for the case of nonequivalent β-methylene protons is studied, the passive coupling effect accentuates the difference in J coupling constant because a large active $^3J_{CO\text{–}H\beta 1}$ coupling invariably combines with a small passive $^3J_{CO\text{–}H\beta 2}$ coupling, and vice versa.

The absolute intensity of an $^nJ_{CO\text{–}H}$ correlation also depends on an additional number of factors. First, presaturation of the H_2O resonance may decrease the amide-proton magnetization via cross relaxation or via exchange of the amide proton with water, thus attenuating the observed correlations correspondingly. Second, ^{15}N and ^{13}CO transverse relaxation times may vary substantially for different amino acids in a protein, significantly affecting the absolute intensity of an observed $^nJ_{CO\text{–}H}$ correlation. Unless both these relaxation rates and the effect of H_2O presaturation are known, it is most prudent to use the relative intensities of the correlations observed for a given amide proton to Hα and Hβ resonances to make a qualitative estimate of the size of the $^3J_{CO\text{–}H\beta}$ coupling. If, for example, a strong correlation to Hα but no correlations to Hβ are observed, this indicates that the CO–Hβ coupling is small. However, if no correlations to either Hα or Hβ are observed, this may be caused by other factors such as broad ^{13}CO or ^{15}N linewidths or H_2O presaturation.

The HN(CO)HB experiment is demonstrated for the protein calmodulin ($M_r \sim 16.7$ kDa) complexed with Ca^{2+}. The experiment was carried out at a 600 MHz ^1H frequency on an unmodified Bruker AMX-600 spectrometer, using a 1.5 mM sample concentration in 95%/5% H_2O/D_2O, pH 6.3, 35°C. On average, ^{15}N transverse relaxation times in the ^1H-coupled mode are ~70 ms, as judged by the ^{15}N linewidth observed in an Overbodenhausen (HSQC) spectrum, and ^{13}CO transverse relaxation times (in the $^1H/^{15}N/^{13}C$-coupled mode) were measured to be ~50 ms. Significant variations of both ^{15}N and ^{13}CO transverse relaxation, however, are present within the protein.

Figure 2 shows sections of two $F_2(^1H)$–F_3(HN) slices taken from the 3D HN(CO)HB spectrum, displaying connectivities between amide and aliphatic protons. As discussed before, the carbonyl nucleus is used for magnetization relay purposes only, and its frequency is not measured in this particular experiment. However, the intensity of a correlation between an amide proton (F_3) and Hα and Hβ protons (F_2) depends primarily on the magnitude of the heteronuclear J coupling between the carbonyl that precedes the observed amide proton and Hα/β (cf. Eq. [7]). For example, on the left side of Fig. 2B, a correlation is observed between the amide proton of Phe-65 and the upfield Hβ' proton of Asp-64; the position of the second Asp-64 proton, Hβ, is marked by the empty box. Clearly, the Hβ' proton is trans relative to the carbonyl, and Hβ is in a gauche position. For Asp-64, the correlation to its Hα proton (at 5.40 ppm) falls outside the window shown but also has very low intensity, indicative of a small $^2J_{CO-H\alpha}$ coupling. For the majority of residues, however, relatively intense correlations via the intraresidue $^2J_{CO-H\alpha}$ are present. For example, all other residues for which correlations are present in Fig. 2 exhibit relatively intense correlations to Hα protons. These resonances all fall in the 3.7–4.4 ppm range and correspond to transfer via $^2J_{CO-H\alpha}$; i.e., they represent correlations between the amide of residue i and Hα of residue i-1.

In the entire 3D spectrum, only 11 intraresidue HN–Hα correlations (via $^3J_{CO-H\alpha}$) were observed and none are present in Fig. 2. An intense intraresidue NH–Hα correlation in the HN(CO)HB spectrum is indicative of a positive ϕ angle near 60°, except for glycines, where ϕ angles of either +60° or −60° are expected to give rise to intense correlations. Four of the eleven observed correlations correspond to glycine residues, G23, G96, G132, and G59; they all have positive ϕ angles in the X-ray crystal structure (*24*) and all four are located in homologous positions in the four calcium-binding loops of calmodulin. For these residues the correlation is observed to the pro-R Hα proton, not to the pro-S proton which replaces Cβ. The remaining intraresidue correlations correspond to residues for which the crystal structure indicates that the Hα is close to a cis arrangement with respect to the carbonyl ($\phi \approx -120°$), or for which ^{15}N relaxation studies indicate a high degree of mobility (*25*).

The HN(CO)HB experiment is considerably more complex than its counterpart, HNHB. In part this is due to the extra magnetization relay step, transferring magnetization via the carbonyl carbon. However, an added degree of difficulty is caused by the fact that the present experiment requires a protein that is highly enriched in both ^{13}C and ^{15}N. Hence, it becomes necessary to remove the effect of both $^1H\alpha/\beta$–$^{13}C\alpha/\beta$, ^{15}N–$^{13}C\alpha$, and ^{13}CO–$^{13}C\alpha$ J couplings. Despite the large number of RF pulses used in the HN(CO)HB experiment, a high-quality spectrum can be recorded in a

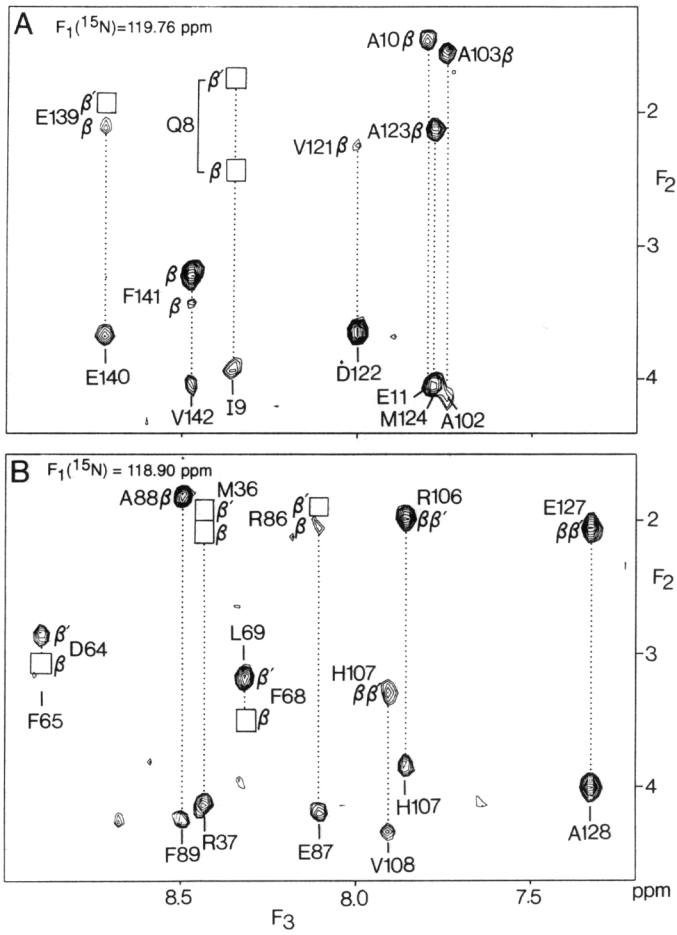

FIG. 2. Two sections of (F_2, F_3) slices taken from the HN(CO)HB spectrum of calmodulin, showing correlations between the amide of one residue (marked below each dotted line) and Hα (unlabeled) and Hβ resonances of the preceding amino acid. Square boxes mark the positions of Hβ protons with vanishing intensity, i.e., with a small $^3J_{CO-H\beta}$. The "invisible" Hβ peak positions have been taken from Ikura *et al.* (*28*). The spectrum results from a (36 complex) × (64 complex) × (512 complex) data matrix, recorded with 128 scans per hypercomplex (t_1, t_2) pair. Acquisition times were 27 ms (t_1, ^{15}N), 12.8 ms (t_2, ^{1}H), and 55.3 ms (t_3, HN). Zero filling and 60°-shifted sine-bell filtering were used in the t_2 dimension and zero filling combined with a squared 60°-shifted sine bell was used for t_3. After t_2 and t_3 Fourier transformation, the t_1 time domain was extended to 72 complex data points using linear prediction with a mirror image constraint (*29*), followed by a squared 90°-shifted sine-bell filter and zero filling to 128 points, prior to the final t_1 Fourier transform.

reasonable amount of measuring time (~3.5 days) using a relatively low sample concentration (1.5 mM) of a protein which is large by NMR standards. The information that it provides is important for determining stereospecific assignments of Hβ methylene protons and χ_1 torsion angles, where it complements other techniques that rely on measurement of Hα–Hβ and ^{15}N–Hβ couplings. In addition, the experiment

provides important sequential NH(i)–Hα(i-1) connectivity information, complementing results obtainable with the H(CA)NNH (*26*) experiment.

ACKNOWLEDGMENTS

This work was supported by the Intramural AIDS Targeted Anti-Viral Program of the Office of the Director of the National Institutes of Health. S.G. acknowledges funding by the Roche Research Foundation.

REFERENCES

1. V. F. BYSTROV, *Prog. NMR Spectrosc.* **10,** 41 (1976).
2. C. GRIESINGER, O. W. SØRENSEN, AND R. R. ERNST, *J. Am. Chem. Soc.* **107,** 6394 (1985).
3. G. T. MONTELIONE, M. E. WINKLER, P. RAUENBUEHLER, AND G. WAGNER, *J. Magn. Reson.* **82,** 198 (1989).
4. G. WAGNER, P. SCHMIEDER, AND V. THANABAL, *J. Magn. Reson.* **93,** 436 (1991).
5. A. S. EDISON, W. M. WESTLER, AND J. L. MARKLEY, *J. Magn. Reson.* **92,** 434 (1991).
6. E. R. P. ZUIDERWEG AND S. W. FESIK, *J. Magn. Reson.* **93,** 653–658 (1991).
7. A. BAX AND M. F. SUMMERS, *J. Am. Chem. Soc.* **108,** 2093 (1986).
8. W. BERMEL, K. WAGNER, AND C. GRIESINGER, *J. Magn. Reson.* **83,** 223 (1989).
9. J. J. TITMAN, D. NEUHAUS, AND J. KEELER, *J. Magn. Reson.* **85,** 111 (1989).
10. J. M. RICHARDSON, J. J. TITMAN, J. KEELER, AND D. NEUHAUS, *J. Magn. Reson.* **93,** 533 (1991).
11. K. V. R. CHARY, G. OTTING, AND K. WÜTHRICH, *J. Magn. Reson.* **93,** 218 (1991).
12. S. J. ARCHER, M. IKURA, D. A. TORCHIA, AND A. BAX, *J. Magn. Reson.*, in press.
13. G. M. CLORE, A. BAX, AND A. M. GRONENBORN, *J. Biomol. NMR* **1,** 13 (1991).
14. L. MUELLER, *J. Am. Chem. Soc.* **101,** 4481 (1979).
15. M. R. BENDALL, D. T. PEGG, AND D. M. DODDRELL, *J. Magn. Reson.* **52,** 81 (1983).
16. A. BAX, R. H. GRIFFEY, AND B. L. HAWKINS, *J. Magn. Reson.* **55,** 301 (1983).
17. M. IKURA, L. E. KAY, AND A. BAX, *Biochemistry* **29,** 4659 (1990).
18. L. E. KAY, M. IKURA, R. TSCHUDIN, AND A. BAX, *J. Magn. Reson.* **89,** 496 (1990).
19. A. BAX, A. F. MEHLKOPF, AND J. SMIDT, *J. Magn. Reson.* **35,** 167 (1979).
20. O. W. SØRENSEN, *J. Magn. Reson.* **90,** 433 (1990).
21. R. POWERS, A. M. GRONENBORN, G. M. CLORE, AND A. BAX, *J. Magn. Reson.* **94,** 209 (1991).
22. F. DELAGLIO, D. A. TORCHIA, AND A. BAX, *J. Biomol. NMR,* in press.
23. P. E. HANSEN, J. FEENEY, AND G. C. K. ROBERTS, *J. Magn. Reson.* **17,** 249 (1975).
24. Y. S. BABU, J. S. SACK, T. J. GREENBOUGH, C. E. BUGG, A. R. MEANS, AND W. J. COOKE, *Nature (London)* **315,** 37 (1985).
25. G. BARBATO, M. IKURA, L. E. KAY, AND A. BAX, unpublished.
26. L. E. KAY, M. IKURA, AND A. BAX, *J. Magn. Reson.* **91,** 84 (1991).
27. D. MARION, M. IKURA, R. TSCHUDIN, AND A. BAX, *J. Magn. Reson.* **85,** 393 (1989).
28. M. IKURA, S. SPERA, G. BARBATO, L. E. KAY, M. KRINKS, AND A. BAX, *Biochemistry,* in press.
29. G. ZHU AND A. BAX, *J. Magn. Reson.* **90,** 405 (1990).